MULTI-PHASE HIGH TEMPERATURE ALLOYS: EXPLORATION OF LAVES PHASE STRENGTHENING OF STEELS

Michael P. Brady
Oak Ridge National Laboratory, Oak Ridge, TN 37831-6115
bradymp@ornl.gov; Tel: (865) 574-5153; FAX (865) 241-0215

C.T. Liu
Oak Ridge National Laboratory, Oak Ridge, TN 37831-6115
liuct@ornl.gov; Tel: (865) 574-4459; FAX (865) 574-7659

Yukinori Yamamoto
Oak Ridge National Laboratory, Oak Ridge, TN 37831-6115
yamamotoy@ornl.gov; Tel: (865) 576-7095; FAX (865) 574-7659

Zhao Ping Lu
Oak Ridge National Laboratory, Oak Ridge, TN 37831-6115
luzp@ornl.gov; Tel: (865) 576-7196; FAX (865) 574-7659

Harry Meyer
Oak Ridge National Laboratory, Oak Ridge, TN 37831-6115
meyerhmiii@ornl.gov; Tel: (865) 574-5092; FAX (865) 576-5413

ABSTRACT

An effort was initiated for the development of intermetallic Laves phase-strengthened Fe-base alloys for improved elevated-temperature strength in fossil energy system components such as superheater tubes and industrial gas turbines. Work in FY 2005 was focused on Al-modified austenitic alloys. Levels of 5 and 8 at.% (2.4 and 3.9 wt.%) Al were sufficient to impart Al_2O_3-based scale formation at 700-800°C in air and air +10% water vapor. Tensile yield strengths for the initial iteration of alloys were in excess of 300 MPa at 750°C. However, creep rupture lives at 750°C and 100 MPa in air were low due to the presence of BCC phase regions in the otherwise austenitic microstructure, their conversion to σ phase, and unoptimized Laves Phase/MC carbide distribution in the microstructure. Modification of alloy composition and processing based on these insights will be pursued in FY2006. Preliminary results suggest that single-phase austenitic microstructures with fine dispersions are possible in Al-modified compositions.

INTRODUCTION

The efficiency of boiler/steam turbine power plants is a strong function of steam temperature and pressure [1]. Consequently, it is attractive to operate at higher temperatures and pressures to increase energy efficiency. However, under such conditions, high-temperature creep strength is a major issue for hot components in advanced fossil energy conversion and combustion systems.

For example, current goals for advanced fossil energy power plants call for ferritic steels capable of operation above 600°C, and austenitic steels capable of operation at greater than 700°C. Components of interest range from superheater tubes to industrial gas turbine components. A key need is the concurrent development of strength and oxidation resistance, especially in oxidizing environments also involving exposure to sulfidation, hot corrosion, or water vapor species.

State-of-the-art ferritic and austenitic steels currently use solid solution strengthening in combination with carbide and/or nitride precipitate strengthening. Significant gains in creep strength have recently been achieved via control of these dispersions at the nanoscale [e.g. 2-4], in some cases achieving strength likely beyond the upper-temperature limit for the alloys set by oxidation in environments containing aggressive species such as water vapor. The current effort is based on multi-phase microstructures utilizing intermetallic phases for high-temperature strengthening and, depending upon the specific alloy system, as a reservoir for protective scale-forming elements. This approach offers a possible path to achieve a balance of properties in Fe-base alloys sufficient to enable increased operating temperatures for applications in aggressive environments encountered in advanced fossil energy power plants.

DISCUSSION OF CURRENT ACTIVITIES

Efforts in FY 2005 were focused on the design of advanced austenitic alloys strengthened by (1) solid solutes, (2) carbide precipitates (MC), and (3) Laves and other intermetallic phase precipitates (Fig. 1). The selection of Laves phases for intermetallic strengthening leverages previous work under the Fossil Energy ARM program on Laves-strengthened Cr and Cr(Fe) alloys [5,6], and recent phase equilibria studies by Takeyama et al. [7], which showed that precipitation of Fe_2Nb-base Laves phase could be controlled in austenitic Fe via manipulation of the Ni content of the alloy. Baseline compositions selected for study were in the range of Fe-(10-20)Cr-(15-25)Ni atomic percent (at.%), with minor additions of elements such as B, C, Mo, Nb, Ti, V, W, etc. The alloys were arc-cast and forged/heat treated, or arc-cast and heat treated. Full compositional and processing details are considered proprietary at this time.

A key goal in FY 2005 was to explore strengthening and oxidation behavior of Al-modified austenitic alloys. Alumina-based scales are of interest due to their superior resistance to water vapor-containing environments, compared to chromia-based scales, which are susceptible to accelerated oxidation due to volatilization-related effects [8]. Al-modified austenitic alloys have been explored intermittently in the past, see for example work by Ramakrishnan et al [9]. Kvernes et al. also reported that as little as 1 wt.% Al was needed in Fe-13Cr base alloys to impart protective alumina scale formation in air + water vapor mixtures at 680°C, while at 980°C 4 wt.% Al was needed [10]. Achieving strengthening in Al-modified austenitic alloys is complicated by (1) the strong BCC stabilizing effects of Al, and potential for δ ferrite formation; (2) possible interference with interstitial nitrogen additions used to enhance strengthening in austenitic alloys (by the formation of AlN); and (3) a tendency to increase stacking fault energy and cross-slip. Therefore, oxidation studies were directed toward assessment of scale formation with relatively low additions of Al, in order to minimize the detrimental effects of Al on strengthening.

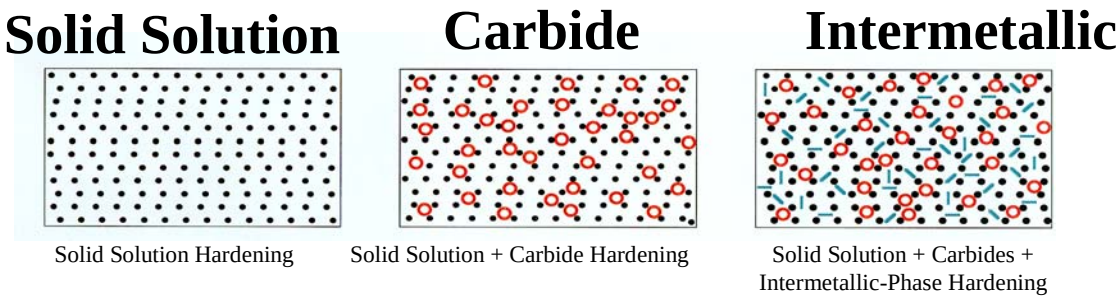

Fig. 1- Schematic representation of superposition of strengthening mechanisms.

Oxidation

Oxidation studies were conducted for Fe-20Cr-15Ni at.% base alloys with 0, 5, and 8 at.% Al (0, 2.4, and 3.9 weight percent Al) in air at 800°C and air + 10% water vapor at 700°C and 800°C. Test samples with dimensions of approximately 12 mm x 18 mm x 1 mm were polished to a 600 grit surface finish. They were placed in alumina holders and exposed for 100-h cycles in the air + water vapor environments and approximately 1-week cycles in laboratory air. Specific weight change vs. time data are shown in Fig. 2.

At 800°C in air (Fig. 2a), the Al-free alloy showed a transition to linear oxidation kinetics between approximately 300 and 700 h of exposure. However, both the 5 and 8 at.% Al alloys showed slow, parabolic-like growth kinetics, consistent with the formation of an alumina-based scale. In air + 10% water vapor at 800°C, the Al-free alloy exhibited a significant degradation of scale protectiveness, and a transition to weight loss between 100 and 200 h of exposure (Fig. 2b). In contrast, the 5 and 8 at.% Al alloys both showed slow, parabolic-like growth kinetics similar to those observed in air. Similar trends were observed at 700°C (Fig. 2c), with the Al-free alloy exhibiting net weight loss after the first 100 h of exposure, and break away oxidation at 800 h of exposure, while the 5 and 8 at.% Al exhibited slow, parabolic-like growth kinetics.

Secondary electron images of cross-sections of the Al-free alloy after 1000 h at 800°C in air, and 500 h at 800°C in air + 10% water vapor, are shown in Fig. 3. In air (Fig. 3a), the scale consisted of an outer layer of a Cr-Fe-Ni-O phase consistent with a spinel phase, and an inner layer rich in Cr_2O_3 (based on SEM/EDS elemental analysis). Similar scale regions were also formed in air + 10% water vapor (Fig. 3 b); however, numerous Fe-rich oxide nodules were also present. Such nodule formation is the acknowledged start of breakdown of Cr_2O_3 in water vapor environments [e.g. 10, 11]. The alloy microstructure consisted of relatively fine, intragranular regions of mixed Fe_2Nb-based Laves phase particles and NbC-based carbides. However, coarse Fe_2Nb/NbC phase regions were also observed at grain boundary regions of the austenitic matrix, as indicated in Fig. 3.

A secondary electron image of a cross-section of the 5 at.% Al alloy after 1000 h at 800°C in air + water vapor is shown in Fig. 4. It consisted of a very thin, Al-rich scale overlying a coarse, duplex austenitic/ferritic microstructure, rather than single-phase austenite. Fine B2 NiAl base precipitates present in the microstructure were denuded underneath the scale, indicating that they acted as a reservoir for the Al-based scale formation. Similar microstructures were observed in

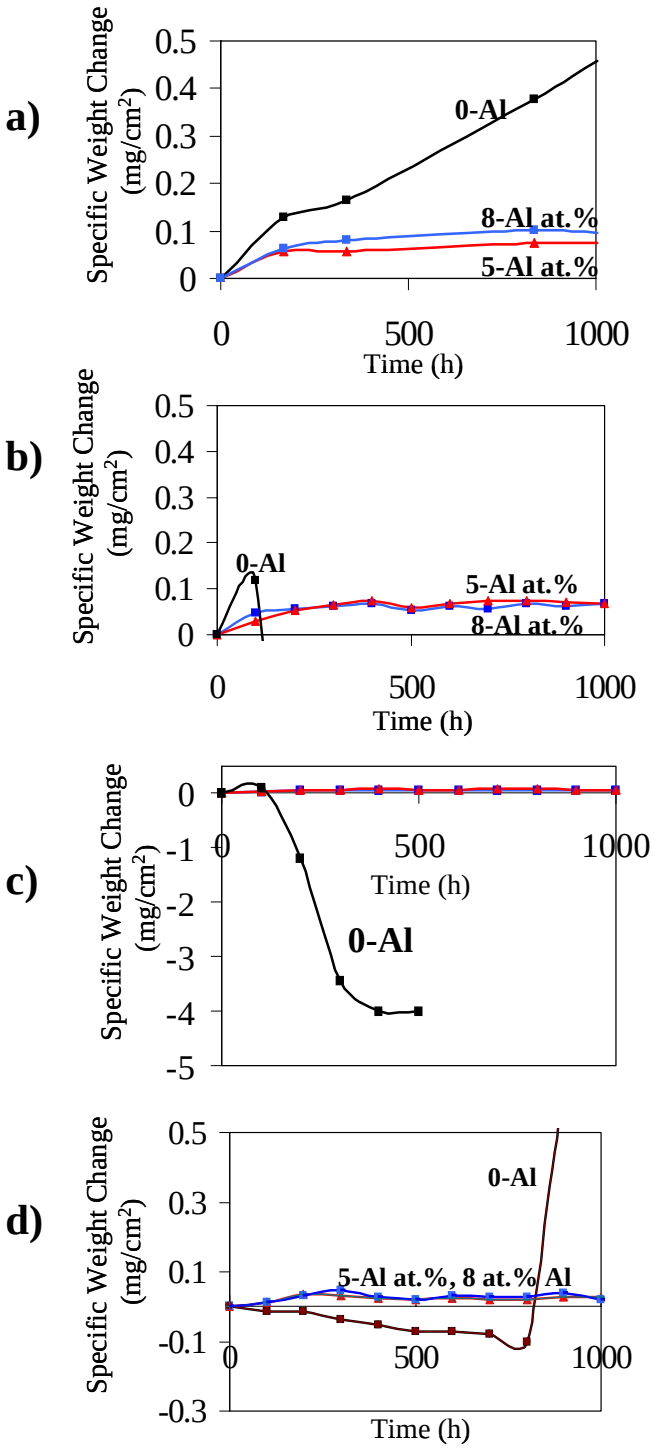

Fig. 2- Oxidation data for Fe-20Cr-15Ni at.% base alloys with 0, 5, and 8 At.% Al.
a) 800°C in air; b) 800°C in air + 10% water vapor; c) 800°C in air + 10% water vapor (full range from (b); d) 700°C in air + 10% water vapor

air, and for the 8 at.% Al alloy in air and air + water vapor. As with the Al-free alloy, both fine intragranular Fe_2Nb/NbC regions and coarse Fe_2Nb/NbC regions were also present. Virtually no coarsening of the fine Fe_2Nb and NiAl precipitates were observed in the 5 at.% Al alloy, even after 1000 h at 800°C, the longest exposure time studied. (NiAl precipitates were observed to coarsen in the 8 at.% Al alloy).

a)

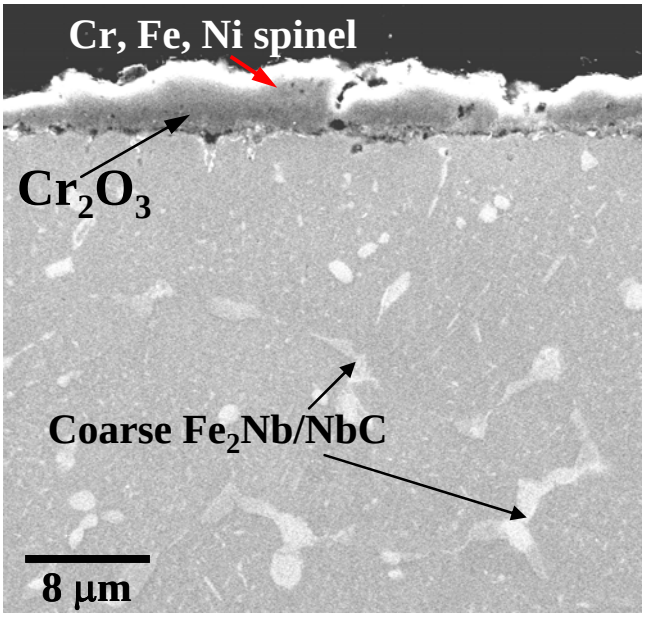

b)

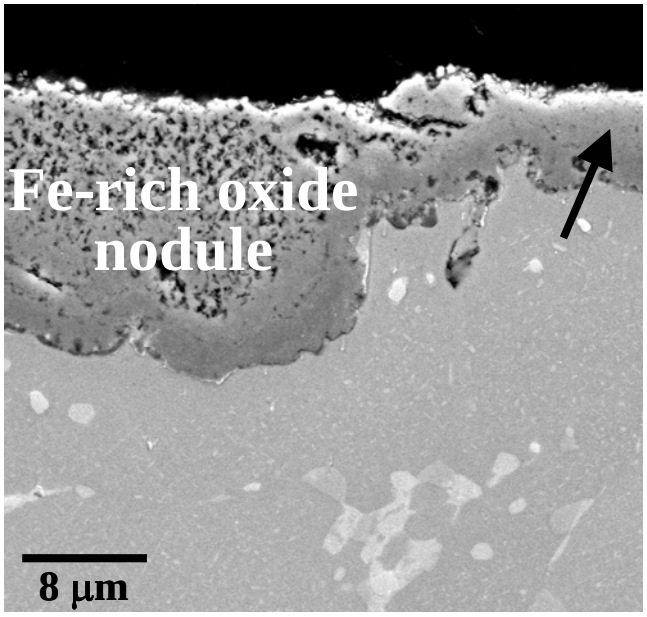

Fig. 3- Secondary electron cross-section images of the Fe-20Cr-15Ni base alloy (0-Al). A) 800°C/1000 h/air; b) 800°C, 500 h, air + 10% water vapor. The arrow in (b) marks a local scale region qualitatively similar to that formed in air (a).

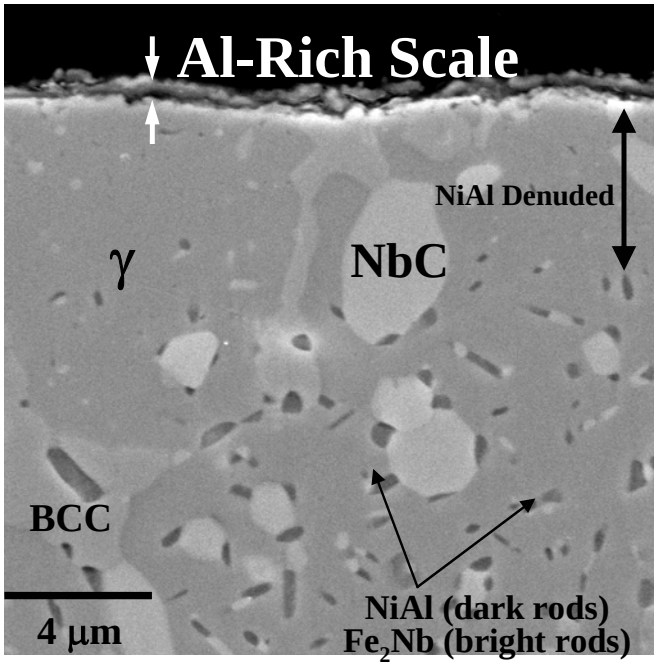

Fig. 4- secondary electron cross-section image of the Fe-20Cr-15Ni-5Al at.% base alloy after 1000 h at 800°C in air + 10% water vapor.

To gain further insight into the nature of the scale, x-ray photoelectron spectroscopy (XPS) and Auger analysis were performed. XPS survey scan data for the 5 at.% Al alloy are shown in Fig. 5a. The surface chemistries were very similar after 1000 h exposure at 800°C in air and air + 10% water vapor. Typical Auger concentration profiles, as a function of sputter time, are shown in Fig. 5b. The scale was Al-rich, but also contained minor quantities of Fe and Cr. Therefore, the surface scale was likely closer to $(Al, Cr, Fe)_2O_3$ than exclusively Al_2O_3. (Note that the oxidized surface was not homogeneous, and that there were some variations in the relative amounts of Fe/Cr and distribution of Fe/Cr within the scale among the different scale spots analyzed). Nb (an alloying addition) and Si and Cu (alloy impurities) were also detected at some locations, as were C, Na, and Cl. X-ray data were consistent with a transition alumina phase, rather than α–Al_2O_3.

Mechanical Properties

Tensile properties and creep rupture resistance were evaluated using subsized, dogbone sheet tensile samples approximately 0.6-0.7 mm thick with a gage length of 12.7 mm. The samples were tested with the as-electro-discharge machined surface finish, using a crosshead speed of 2.54 mm/minute (strain rate of $3.33\ 10^{-3}$/s).

Tensile properties for several Al-modified developmental alloys are summarized in Table 1. At room temperature, yield strengths were in excess of 700 MPa, and elongation was in the range of 5%. At 700°C, yield strength decreased relative to room temperature, but was still in excess of 400 MPa, and elongations ranged from 25-70%. At 750°C, yield strengths were in the 280-380

MPa range, with elongations of 50 –80%. These results indicate that appreciable tensile elongations are possible for steels with Fe_2Nb Laves phase and NiAl precipitates.

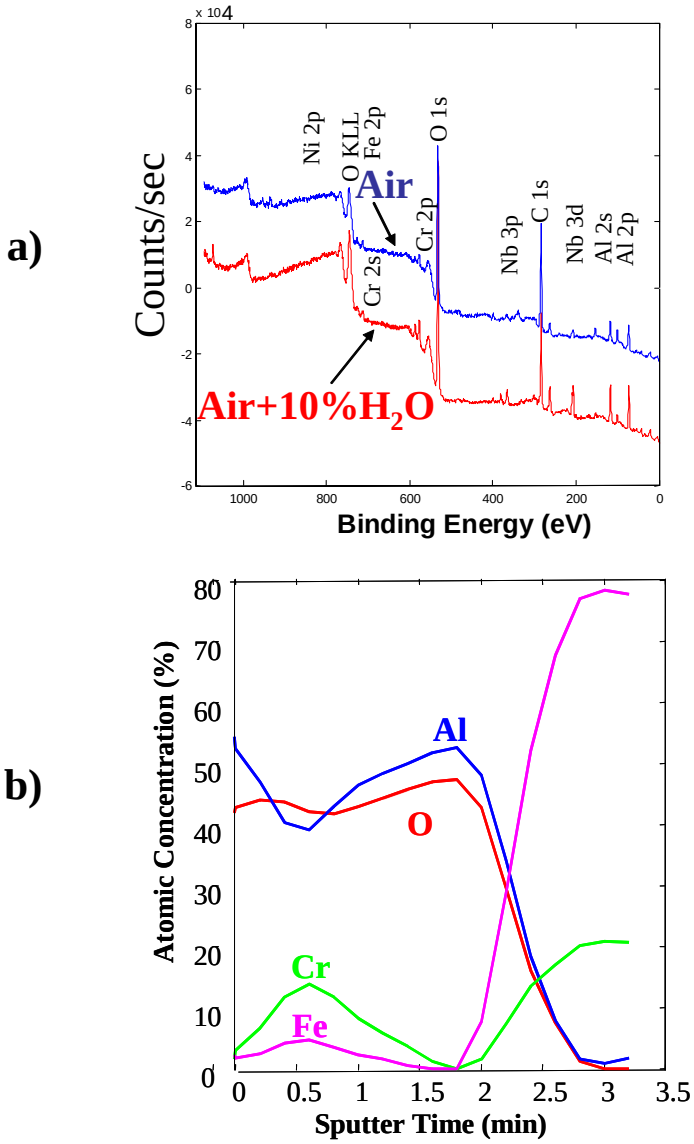

Fig. 5: Surface chemistry for the Fe-20Cr-15Ni-5Al at.% base alloy after 1000 h at 800°C in air + 10% water vapor. a) XPS survey scans (includes control data for 1000 h oxidation in air); b) Auger sputtering profile

Table 1- Tensile properties of Fe-20Cr-15Ni at.% base alloys with 8, 6.5, and 5 at.% Al, respectively. Minor additions of Nb, C, B, Mo, etc. were also present.

Alloy No.	Yield (ksi, MPa)	Tensile Fracture (ksi)	Elongation (%)
Room Temperature			
8 at.% Al	122 (840)	141	5.1
6.5 at.% Al	113 (780)	132	4.7
5 at.% Al	102 (700)	121	6.6
700°C			
8 at.% Al	52.0 (360)	44.5	68.1
6.5 at.% Al	62.6 (430)	84.2	26.5
5 at.% Al	60.0 (414)	82.4	40.5
750°C			
8 at.% Al	41.2 (284)	51.9	81.8
6.5 at.% Al	51.0 (352)	65.5	58.8
5 at.% Al	54.3 (375)	76.1	48.3

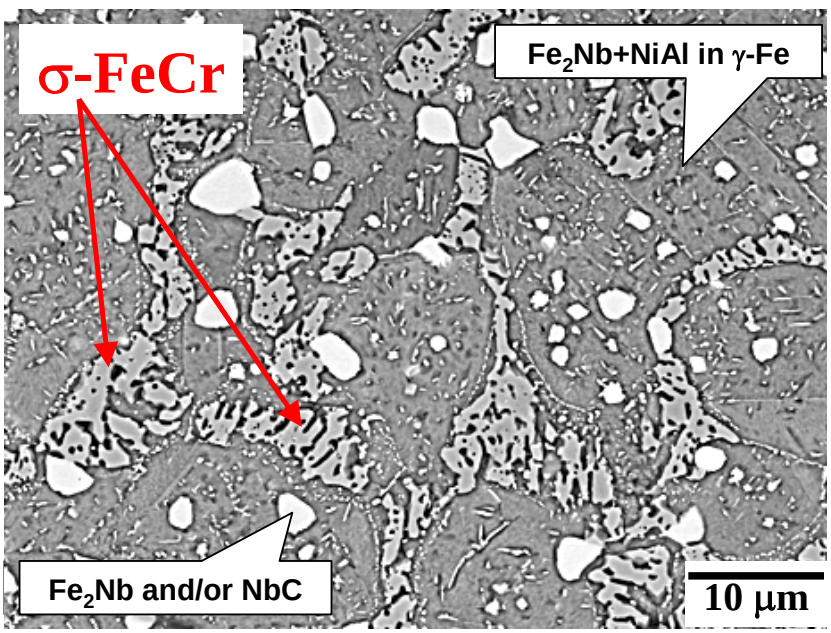

Fig. 6: Secondary electron image of typical Fe-20Cr-15Ni-5Al at.% alloy after creep-rupture life testing at 750°C and 100 MPa in air.

Despite the high levels of yield strength, creep assessment at 750°C and 100 MPa in air indicated relatively poor behavior, with rupture in the range of 10-48 h. For comparison, MC-carbide optimized advanced austenitics can exhibit creep-rupture lives of several thousand hours under these test conditions [3,4]. Post-creep test microstructural analysis indicated that the BCC phase regions in the Al-modified alloys converted to σ phase during the course of the creep test (Fig. 6). The low creep-rupture lives were attributed to the presence of BCC phase regions in the

microstructure, and their conversion to σ phase, combined with the relatively fine matrix grain size and coarse dispersion of Fe_2Nb/NbC-based phases (Fig. 4). However, as shown in Fig. 7, fine dispersions of Laves Fe_2Nb and B2 NiAl phases were also formed in some intragranular austenitic regions. These precipitates showed no appreciable coarsening on ageing at 800°C for 1000 h. Therefore, with further optimization of alloy composition and processing, the possibility exists in these alloys to form γ microstructures with fine, stable dispersions, with the potential for improved creep resistance over levels currently achieved.

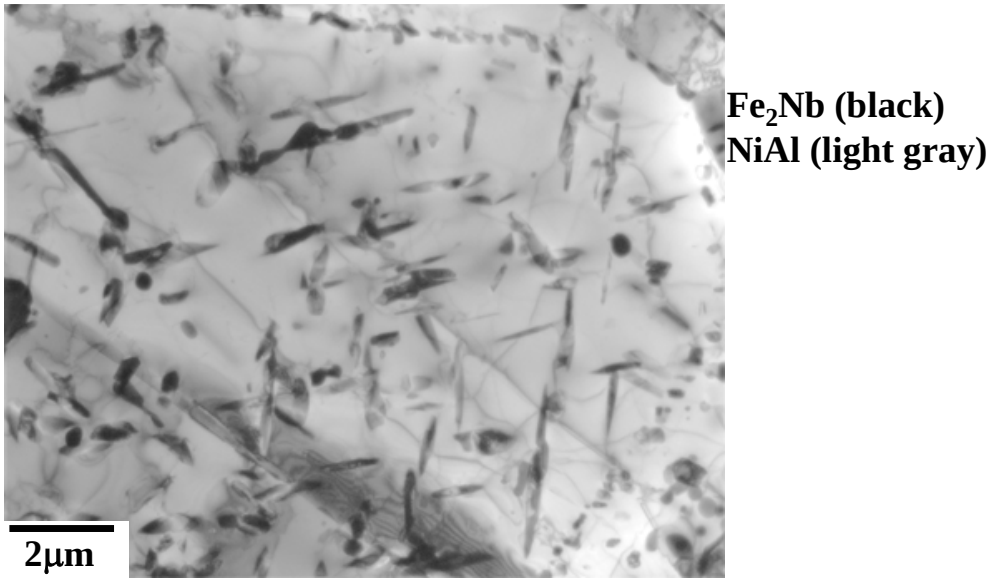

Fig. 7: Transmission electron microscopy bright field image of 800°C aged Fe-20Cr-15Ni-5Al at.% base alloy showing γ matrix intragranular region containing fine Fe_2Nb and NiAl base precipitates.

FUTURE WORK

The first iteration of Al-modified austentic alloys showed a promising combination of oxidation resistance in air + water vapor environments and room-temperature and elevated-temperature tensile properties. To eliminate the BCC regions that degraded creep rupture life, modification in Ni and Cr levels will be made to ensure a single-phase austenitic matrix. Grain size will be controlled through hot fabrication and heat treatment. Modification in alloying addition levels of Nb is also needed to refine the Fe_2Nb and NbC base phase precipitates, and eliminate the coarse intergranular regions. Preliminary microstuctural analysis of a new iteration of alloys incorporating these changes suggests that such microstructures are possible in alloys with 5 at.% Al. Work in FY 2006 will also focus on determination of creep strengths with alloys solely containing Laves phase dispersions (no carbon additions/carbides), based on Takeyama et al [7], to definitively assess the potential of using Fe_2Nb-based Laves phases to strengthen austenite.

REFERENCES

1. R. Viswanathan and W. Bakker, *J. Mat. Eng. Perf.*, 10 (1), 81 (2001).

2. R.L. Klueh, N. Hashimoto and P.J. Maziasz, *Scripta Mater.*, 53 (3), 275 (2005).

3. P.J. Maziasz, J.P Shingledecker, R.W. Swindeman, R.L. Klueh and N.D. Evans, *18th Annual Conf on Fossil Energy Mtls, Knoxville, TN USA, Fossil, Oak Ridge National Laboratort, Oak Ridge, TN USA, 06/02/2004-06/04/2004*.

4. T. Sourmail, *Mater. Sci Tech.*, 17 (1), 1 (2001).

5. M.P. Brady, J.H. Zhu, C.T. Liu, P.F. Tortorelli, L.R. Walker, C.G. McKamey, J.L. Wright, C.A. Carmichael, D.J. Larson, M.K. Miller, and W.D. Porter, *Mater. High Temp.*, 16(4), 189 (1999).

6. M.P. Brady, C.T. Liu, J.H. Zhu, P.F. Tortorelli, and L.R. Walker, *Scripta Mater.*, 52, 9, 815 (2005).

7. M. Takeyama, S. Morita, A. Yamauchi, M. Yamanaka, and T. Matsuo, in Superalloys 718, 625, 706 and Various Derivatives, E.A. Loria, Ed., TMS 2001 p. 333.

8. E.J. Opila, *Mater. Sci. For*., 461-464, 765 (2004).

9. V. Ramakrishnan, J.A. Mcgurty, N. Jayaraman, *Oxid. Met*., 30 (3-4), 185 (1988).

10. I. Kvernes, M. Oliveira, and P. Kofstad, *Corr. Sci.* , 17, 237 (1977).

11. B.A. Pint, R. Peraldi, P.J. Maziasz, PJ, *Mater. Sci. For*., 461-464, 815 (2004).

ACKNOWLEDGEMENTS

This research was sponsored by the U.S. Department of Energy, Fossil Energy Advanced Research Materials (ARM) Program. Oak Ridge National Laboratory is managed by U.T.-Battelle, LLC for the U.S. Department of Energy. The authors thank Bruce Pint, Peter Tortorelli, and Ian Wright for reviewing this manuscript. Extensive discussions and technical input from Phil Maziasz, Bruce Pint, John Shingledecker, and Ian Wright are also gratefully acknowledged